Plasma proteome profiling of healthy subjects undergoing bed rest reveals unloading-dependent changes linked to muscle atrophy

Marta Murgia[1,2]* , Lorenza Brocca[3], Elena Monti[1], Martino V. Franchi[1,4], Maximilian Zwiebel[2], Sophia Steigerwald[2], Emiliana Giacomello[5], Roberta Sartori[1,6], Sandra Zampieri[1,4,7], Giovanni Capovilla[7], Mladen Gasparini[8], Gianni Biolo[5], Marco Sandri[1,6], Matthias Mann[2,9] & Marco V. Narici[1,4]

[1]*Department of Biomedical Sciences, University of Padova, Padua, Italy;* [2]*Max-Planck-Institute of Biochemistry, Martinsried, Germany;* [3]*Department of Molecular Medicine, University of Pavia, Pavia, Italy;* [4]*CIR-MYO Myology Center, Padua, Italy;* [5]*Department of Medicine, Surgery and Health Sciences, University of Trieste, Trieste, Italy;* [6]*Veneto Institute of Molecular Medicine, Padova, Italy;* [7]*Department of Surgical, Oncological and Gastroenterological Sciences, Padova University Hospital, Padua, Italy;* [8]*Izola General Hospital, Izola, Slovenia;* [9]*NNF Center for Protein Research, Faculty of Health Sciences, University of Copenhagen, Copenhagen, Denmark*

Abstract

Background   Inactivity and unloading induce skeletal muscle atrophy, loss of strength and detrimental metabolic effects. Bed rest is a model to study the impact of inactivity on the musculoskeletal system. It not only provides information for bed-ridden patients care, but it is also a ground-based spaceflight analogue used to mimic the challenges of long space missions for the human body. In both cases, it would be desirable to develop a panel of biomarkers to monitor muscle atrophy in a minimally invasive way at point of care to limit the onset of muscle loss in a personalized fashion.

Methods   We applied mass spectrometry-based proteomics to measure plasma protein abundance changes in response to 10 days of bed rest in 10 young males. To validate the correlation between muscle atrophy and the significant hits emerging from our study, we analysed in parallel, with the same pipeline, a cohort of cancer patients with or without cachexia and age-matched controls. Our analysis resulted in the quantification of over 500 proteins.

Results   Unloading affected plasma concentration of proteins of the complement cascade, lipid carriers and proteins derived from tissue leakage. Among the latter, teneurin-4 increased 1.6-fold in plasma at bed rest day 10 (BR10) compared with BR0 (6.E9 vs. 4.3E9, $P = 0.02$) and decreased to 0.6-fold the initial abundance after 2 days of recovery at normal daily activity (R + 2, 2.7E9, $P = 3.3E-4$); the extracellular matrix protein lumican was decreased to 0.7-fold (1.2E9 vs. 8.5E8, $P = 1.5E-4$) at BR10 and remained as low at R + 2. We identified six proteins distinguishing subjects developing unloading-mediated muscle atrophy (decrease of >4% of quadriceps cross-sectional area) from those largely maintaining their initial muscle mass. Among them, transthyretin, a thyroid hormone-binding protein, was significantly less abundant at BR10 in the plasma of subjects with muscle atrophy compared with those with no atrophy (1.6E10 vs. 2.6E10, $P = 0.001$). Haptoglobin-related protein was also significantly reduced in the serum of cancer patients with cachexia compared with that of controls.

Conclusions   Our findings highlight a combination or proteomic changes that can be explored as potential biomarkers of muscle atrophy occurring under different conditions. The panel of significant proteomic differences distinguishing atrophy-prone and atrophy-resistant subjects after 10 days of bed rest need to be tested in a larger cohort to validate their potential to predict inactivity-triggered muscle loss in humans.

Keywords   Proteomics; Plasma; Skeletal muscle; Bed rest; Atrophy; Cachexia

Introduction

Muscle atrophy can be triggered by immobility and nutrients deprivation and is a severe co-morbidity for patients suffering from debilitating chronic diseases or undergoing long hospitalizations.[1] Sarcopenia is a crucial factor in the loss of autonomy of the elderly population and, together with weight loss, is part of the diagnostic criterion for cancer cachexia,[2] a multifactorial syndrome associated with poor outcomes in cancer patients.[3]

Atrophy causes detrimental changes to the morphology and function of skeletal muscles. The onset of muscle atrophy caused by unloading is observed in just 2 days[4] accompanied by alterations of contractile properties within the same timeframe.[5,6] This atrophic state develops when hyperactivation of proteolysis and organelle degradation exceed rates of protein synthesis and organelle biogenesis. Proteolysis occurs via calcium-dependent proteolytic pathways and ubiquitin-mediated proteasomal and autophagic lysosomal processes. These are potentiated when cellular signalling events promote transcription of genes controlling protein degradation, which are controlled by Forkhead box protein O (FoxO)-dependent pathways.[7,8] FoxO dephosphorylation induces the ubiquitin proteasome system through the activation of E3 ubiquitin ligases[9,10] and can directly enhance the autophagy system.[11] Mitochondrial alterations (for instance, mitochondrial fusion/fission machinery imbalance)[12] and reactive oxygen species (ROS) can activate FoxO pathways as well as systemic signals, such as the pro-inflammatory cytokines IL1, IL6 and TNFα and myostatin.[13]

As muscles are the major site of glucose uptake through glucose transporter type 4 (GLUT4), and the largest amino acid reservoir,[14] loss of muscle mass has systemic consequences on metabolism. Blood plasma, by circulating through all organs, is expected to relay this information dynamically, through changes in the abundance of its ions, small molecules and protein composition. With this in mind, we set out to use plasma proteomics as a tool to convey first-hand information on skeletal muscle trophism and monitor muscle atrophy. Our goals were to provide a system view of the changes caused by muscle atrophy to the plasma proteome and to highlight single proteins and protein signatures whose plasma abundance correlates with the loss of muscle mass. If a pool of plasma biomarkers of muscle atrophy existed, one could use a minimally invasive 'liquid biopsy' to monitor muscle mass at point of care, in combination with indirect proxies such as body weight and grip strength. This would be instrumental for frail sarcopenia patients as well as for astronauts during long space missions on the International Space Station, where they experience severe muscle atrophy and loss of force despite intensive physical training on board.[15]

To this aim, we used state-of-the-art mass spectrometry (MS)-based proteomics to analyse the blood plasma of a cohort of 10 young healthy subjects undergoing 10 days of continuous bed rest. In the same cohort, we had analysed in parallel muscle atrophy in great detail, showing a median 5.2% loss of the quadriceps volume and 13% of maximum isometric voluntary contraction of the knee extensors.[16] We here measure the plasma proteome of these subjects before bed rest (BR0) and at the endpoint of the unloading phase at day 10 (BR10). Our data reveal changes in the abundance of 34 proteins after 10 days of bed rest, comprising both canonical plasma components and proteins possibly originating from tissue leakage. Our parallel analyses had unexpectedly shown that three subjects in our cohort were largely resistant to bed rest-induced muscle atrophy, whereas the other seven had lost both mass and force at BR10. Exploring this serendipitous observation, we could find proteins distinguishing the plasma proteome of subjects undergoing no or minor muscle atrophy from that of subjects undergoing extensive atrophy after 10 days of bed rest.

To carry out an initial validation of our findings, we analysed by MS-based proteomics the serum of a second cohort comprising gastrointestinal cancer patients, with and without cachexia, and age-matched patients hospitalized for non-neoplastic diseases. Although muscle atrophy is a common feature, there are profound differences between the two cohorts. However, it is well established that various types of atrophy share a common set of transcriptional adaptations acting through the regulation of proteasome activity. FoxO-controlled atrophy-related genes were discovered as commonly regulated in conditions as diverse as cachexia, starvation, diabetes and kidney disease.[13]

Aiming at downstream common changes, in line with previous studies,[17] we thus explored by proteomics two conditions causing skeletal muscle atrophy. We highlight a group of potential biomarkers that can be explored for their correlation to muscle atrophy in different pathological states.

Methods

Patient cohorts

The bed rest study was approved by the National Ethical Committee of the Slovenian Ministry of Health on 17 July 2019, with reference number 0120-304/2019/9. The study involving cancer patients was approved by the Ethical Committee for Clinical Experimentation of Provincia di Padova (protocol number 3674/AO/15). The bed rest cohort has been previously described.[16] Ten young healthy volunteers (*Table* S1) were housed in a horizontal lying position for 10 full days in standard hospital rooms without interruption and were not allowed to carry out any form of exercise on their beds. They were given an individually controlled eucaloric diet during the whole hospital stay. Blood was sampled right before the begin of bed rest (BR0), at day 10

right before the subject was allowed to stand up (BR10). We also analysed plasma drawn after 2 days of monitored recovery in the hospital (R + 2). This was the endpoint of the study carried out under strictly controlled diet and activity conditions, after which the subjects were discharged from the hospital. We used part of a cachexia cohort, which has been previously described.[18] Patients were stratified into 'cachectic' and 'pre-cachectic' subgroups[2] and compared with patients undergoing surgery for non-neoplastic noninflammatory diseases (control). The subgroup of patients from that cohort used in this study is described in *Table* S2.

Plasma and serum sample processing

The 12 most abundant plasma protein components comprise about 95% of the total protein mass, making the quantification of proteins in the low abundance range extremely challenging.[19] We therefore used a highly sensitive analytical workflow, with one-buffer sample preparation combined with novel MS acquisition modes and computational methods. For peptide preparation, 5 μl of plasma or serum was diluted in 50 μl of LYSE buffer (PreOmics), heated at 95°C for 5 min and sonicated in a water-bath sonicator (Diagenode) for 5 min with a 50% duty cycle. Proteolytic digestion was carried out by addition of 2 μg of endoproteinase LysC and 2 μg of trypsin. After overnight digestion at 37°C under continuous shaking, samples were acidified to a final concentration of 0.1% trifluoroacetic acid (TFA) and loaded onto StageTip plugs of SDB-RPS. Purified peptides were eluted with 80% acetonitrile-1% ammonia and dried. For the library used for match between runs (see below) peptides from all samples were pooled and eluted into 24 fractions using a Spider Fractionator. Concentration of HDL, LDL cholesterol and triglycerides was measured in plasma of bed rest subjects using an automated hospital clinical chemistry pipeline. Contamination from erythrocytes, platelets and coagulation factors was calculated using a custom-made R script based on an online resource (www.plasmaproteomeprofiling.org) derived from recent findings.[20]

Liquid chromatography and tandem mass spectrometry

Peptides were separated on 50-cm columns (75 μm inner diameter) of ReproSil-Pur C18-AQ 1.9 μm resin (Dr Maisch GmbH) packed in-house. The columns were kept at 60°C using a column oven. Liquid chromatography–mass spectrometry (LC-MS) analysis was carried out on an EASY-nLC-1200 system (Thermo Fisher Scientific) coupled through a nanoelectrospray source to a mass spectrometer. Samples were analysed in technical triplicates. Samples S8–S10 at time R + 2 were analysed in technical duplicates. For the bed rest

cohort, the analysis was carried out on a Q Exactive HF mass spectrometer (Thermo Fisher Scientific). Peptides were loaded in buffer A (0.1% (v/v) formic acid) applying a non-linear 45-min gradient of 3–75% buffer B (0.1% (v/v) formic acid, 80% (v/v) acetonitrile) at a flow rate of 450 nL/min. For the cancer patient cohort, samples were analysed on an Orbitrap Exploris 480 mass spectrometer (Thermo Fisher Scientific). Peptides were loaded in buffer A applying a non-linear 120-min gradient of 0–65% buffer B at a flow rate of 300 nL/min. Data acquisition switched between a full scan and 15 data-dependent tandem mass spectrometry (MS/MS) scans. Multiple sequencing of peptides was minimized by excluding the selected peptide candidates for 30 s.

Computational proteomics and data deposition

The MaxQuant software (versions 1.6.10.43 and 2.0.3.0) was used for the analysis of raw files searching against the human UniProt databases (UP000005640_9606, UP000005640_9606_additional) and a common contaminants database.[21] The false discovery rate (FDR) was set to 1% for peptides and proteins and was determined by searching a reverse database. Peptide identifications by MS/MS were matched between the samples and the library files with a 0.7-min retention-time match window. Peptides with a minimum length of seven amino acids were considered for the search including N-terminal acetylation and methionine oxidation as variable modifications and cysteine carbamidomethylation as fixed modification. Enzyme specificity was set to trypsin cleaving C-terminal to arginine and lysine. A maximum of two missed cleavages was allowed. In our dataset, the number of quantified peptides per proteins varied from 258 (Apolipoprotein B) to 1. In the bed rest dataset, of the 44 proteins out of 535 that were quantified with only one peptide, only teneurin-4 (TENM4, 112 MS/MS quantifications) was considered for further analysis. All other proteins quantified with only one peptide were not further analysed. The MS-based proteomics data have been deposited to the ProteomeXchange Consortium via the PRIDE partner repository with the dataset identifier PXD032969 and are publicly available as of the date of publication.

Bioinformatic and statistical analysis

Analyses were performed with the Perseus software (version 1.6.15.0), part of the MaxQuant environment[22] and with the R software environment (https://www.R-project.org). Label-free quantification values with a minimum ratio of 1 were used throughout the analysis for protein abundance using the feature implemented in MaxQuant.[23] Categorical annotations were supplied in the form of UniProt Keywords, Corum, KEGG and Gene Ontology terms. Annotation enrichments

were calculated by Fisher's exact test using the Benjamini–Hochberg method for FDR truncation at a cutoff of 2% and the UniProt human proteome as background. For longitudinal comparisons, we used paired Student's *t*-tests, with significance threshold set at 5% using permutation-based FDR with 250 randomizations. Technical replicates were averaged ($N = 10$). For comparison between different subjects within both cohorts, we used Welch tests with significance cut-off set at 5% employing permutation-based FDR with 250 randomizations and one-way ANOVA ($P < 0.05$) with Tukey's honestly significant difference post hoc tests. Principal component analysis (PCA) was carried out after filtering the dataset for 60% valid values and imputing missing values, assuming a Gaussian distribution and with a downshift of 1.8 the standard deviation of valid values.

Results

Proteomic workflow and features of the bed rest plasma dataset

We carried out a longitudinal proteomic analysis of the blood plasma of 10 young healthy volunteers undergoing ten days of continuous bed rest (*Tables* S1 and S3). Samples were taken immediately before bed rest (BR0), at day 10 (BR10) and after 2 days of free re-ambulation post bed rest (R + 2). Our second cohort consisted of 14 cancer patients, seven with cachexia and seven without, and 14 controls (*Tables* S2 and S4). All samples were analysed by liquid chromatography coupled to MS/MS followed by computational analysis. The two datasets were measured separately and the protein abundance results were cross-analysed (*Figure* 1A; see also Materials and methods).

Our proteomic analysis of the bed rest cohort resulted in an average Pearson correlation of 0.95 among all subjects and time points without clear outliers and of >0.96 for technical replicates (*Figure* S1A). We quantified 535 proteins in total and 360 per subject on average, of which 286 were quantified in all subjects (*Figure* S1B). We carried out a quality control assessment of our plasma samples by measuring the intensities of known marker proteins from three contamination panels, derived from other blood components and occurring in plasma due to improper sample handling.[20] Contamination from red blood cells was consistently below a recommended intensity threshold of 2.5% (*Figure* S1C) and from platelets below 0.5% (*Figure* S1D). Coagulation markers were mostly below 10% in all samples, except for triplicates of one subject at one time point (28%), likely resulting from incorrect sample handling (*Figure* S1E).

The quantitative dynamic range of intensity in our plasma dataset spans five orders of magnitude from highly abundant albumins to the lowest intense protein quantified, the cytoskeleton-associated protein Profilin-1. We crossed our plasma dataset to the 'secreted to blood' protein list of the Human Protein Atlas, containing 784 proteins.[24] Proteins in the highest expression quartile predominantly originated from plasma. Proteins of other origin, possibly deriving from tissue leakage, were progressively more prevalent in the lower intensity quartiles. We could detect nuclear and mitochondrial proteins, likely deriving from cell damage (*Figure* 1B). The highest intensity quartile 1 was significantly enriched in GO terms of apolipoproteins and acute-phase proteins, whereas the lowest quartile 4 was enriched in intracellular proteins, indicating a tissue leakage origin (*Figure* 1C).

To verify that unloading was the major source of variability within the samples, we carried out PCA. This procedure separated the BR0 (black squares) from the BR10 (orange dots) samples diagonally along components 1 and 2 (*Figure* 1D), based on differences in both canonical plasma proteins, like APP and SERPINA1, and tissue leakage proteins, like the mitochondrial ATP5B and the chaperone HSP90AB1 (*Figure* 1E). This result shows that the differences in the plasma proteome correlating with unloading are larger than the individual variability among subjects. Samples taken at R + 2 were clearly separated by PCA from both BR0 and BR10 (*Figure* S1F,G).

Loading-dependent changes in the plasma proteome

Blood was drawn from all subjects right before bed rest (BR0), after 10 days of continuous bed rest (BR10) and 2 days after re-ambulation (R + 2) before hospital discharge. We constructed a global correlation map containing pairwise relationships between all proteins quantified in the dataset. In our case, there were up to 87 abundance values for each plasma protein (10 individuals; three time points, two to three technical replicates). Unsupervised hierarchical correlation clustering of the expression profiles across all samples yielded clusters of highly co-regulated proteins (cluster mean >0.8) involved in the immune response, complement and coagulation cascades, lipid metabolism and integrin signalling (*Figure* S2).

To highlight proteins whose abundance in plasma changes at the different loading states of this sequence, we compared samples taken in the unloading phase (BR10) with those drawn in the loading phase pre-bed (BR0) and post-bed rest (R + 2). We carried out paired *t*-tests for all 10 subjects and three technical replicates, retrieving 22 proteins with significantly different abundance between BR10 and BR0 and 32 between BR10 and R + 2. Unsupervised hierarchical clustering of the median expression of these proteins in 10 subjects grouped the plasma at BR0 and R + 2, separating it from that at BR10. Eight proteins were significant hits in both comparisons. (*Figure* 2A and *Table* S5). The plasma proteins whose
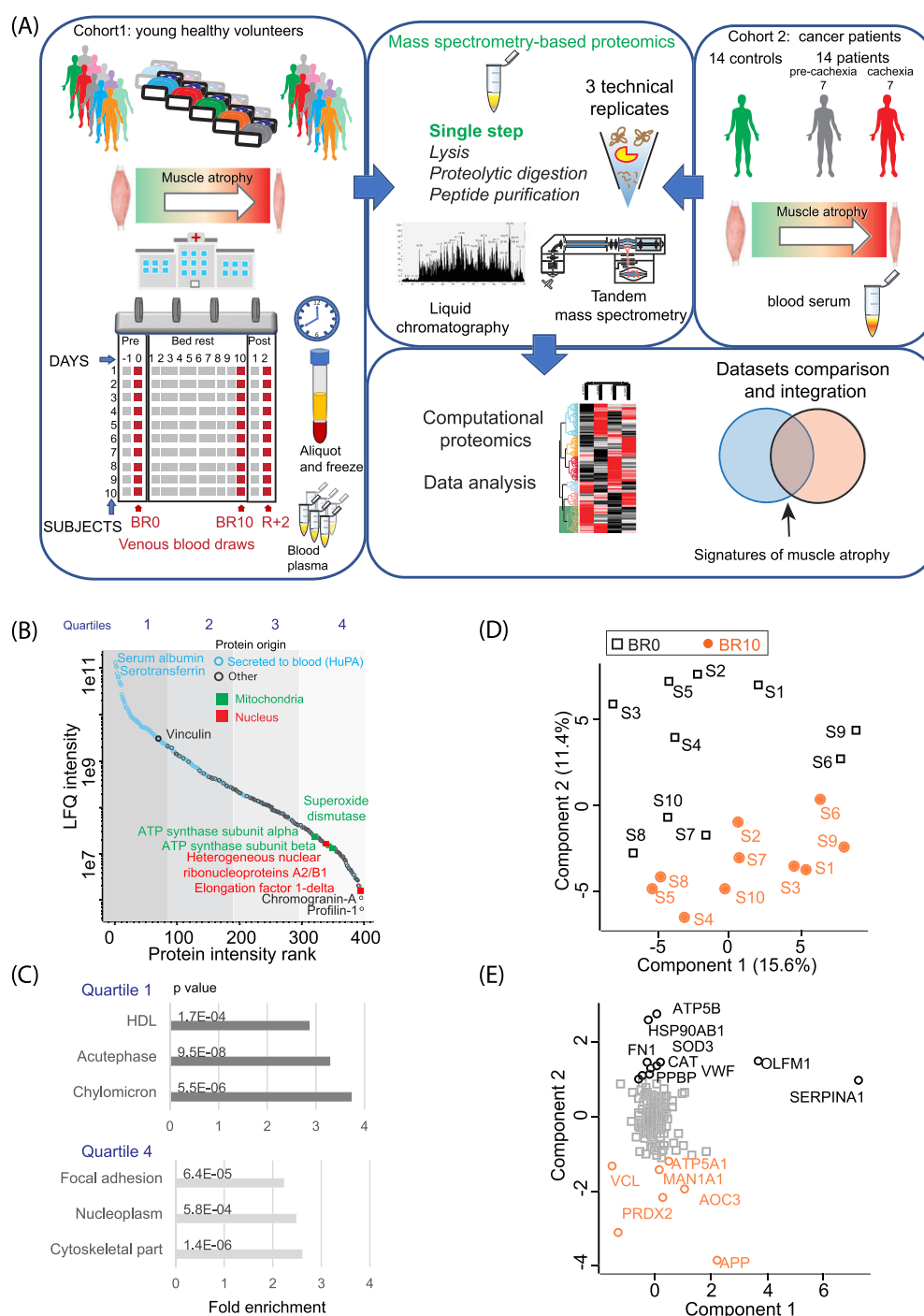
Figure 1 Study design and main features of the dataset. (A) Sample collection, preparation and proteomic analysis workflow. The study cohort involved 10 subjects who underwent 10 days of continuous bed rest that caused muscle atrophy. BR0, before bed rest. BR10, after 10 days of continuous bed rest, R + 2, after 2 days of recovery at weight-bearing conditions. A second cohort used for validation comprised serum from 14 cancer patient with or without cachexia and 14 controls. Frozen samples were proteolytically digested and analysed by liquid chromatography coupled to mass spectrometry, followed by computational proteomics and data analysis. (B) Intensity rank of the proteins quantified in the plasma of the subjects at three time points. Proteins in light blue are annotated as 'secreted to blood', a list of 784 proteins in the Human Protein Atlas (HuPA) repository. The two most and least abundant proteins are labelled. Representative proteins derived from intracellular compartments are marked over the abundance range (red and green squares). Abundance quartiles are visualized with different shades of grey. (C) Top annotation enrichments among highly abundant proteins in the first quartile (top) among low abundance proteins in the fourth quartile (bottom). Fisher exact test, Benjamini–Hochberg FDR for truncation with threshold set at 0.02. (D) Principal component analysis (PCA) separating the plasma proteome of 10 subjects at BR0 (black squares) from that at BR10 (orange dots). (E) PCA loadings, with the proteins driving the separation between the groups labelled in the corresponding colours.

abundance changes significantly between different loading states can be assigned several distinct functions. Most proteins were annotated to GO terms blood coagulation, immunity and lipid transport (*Figure* 2B). Four hits, namely, Lumican, Teneurin 4, Proteoglycan 4 and IgGFc-binding proteins, were not among the plasma-secreted to blood gene set. Based on their characterized interactors (STRING, see Supporting Information), they may be interacting with the extracellular matrix, and one of them, Teneurin4, has a synaptic localization.[25] Proteoglycan4/Lubricin is a lubricating glycoprotein localized at the cartilage surface with a key function in the biomechanical properties of the tissue[26] (*Figure* 2C).

We confirmed the decreased abundance of Lumican in plasma during bed rest by western blot, analysing also an intermediate timepoint of the sequence, BR5. Our results showed a consistently higher Lumican signal in the plasma from BR0 in all subjects analysed with this method, matching the results obtained by MS-based proteomics (*Figure* 2D). Depletion from plasma of the 12 most abundant proteins allowed a clearer visualization of this effect (*Figure* 2D, right panel).

Functional interaction networks of plasma proteins changing in abundance with body loading state

We divided the plasma proteins significantly changing in abundance between body loading states into two groups, namely proteins with (i) lower abundance at BR10 and (ii) higher abundance at BR10 unloading compared with both BR0 and R + 2. We then visualized both groups as functional interaction networks, based on physical interaction, co-expression and data mining (see Supporting Information). Proteins whose abundance in plasma decreased significantly during bed rest and increased again upon reloading included proteins involved in coagulation and were significantly enriched in the annotation term extracellular matrix organization (*P* = 1.4E-5) (*Figure* 3A). We calculated the BR10/BR0 abundance ratio in each of the 10 subjects separately. The decrease in abundance could be measured in a majority of subjects for most proteins, and it was especially large (>4-fold) in the case of fibronectin, platelet basic protein and von Willebrand factor (*Figure* 3B). Proteins whose abundance increased at BR10 compared with both BR0 and R + 2 formed a tight functional network specifically enriched in the annotation term protease inhibitor (*P* = 2.5E-10) and lipoproteins (*P* = 2.7E-8) (*Figure* 3C). The latter might be correlated with the changes in lipid metabolism measured in these subjects during bed rest, which included a decrease in plasma cholesterol and an increase in triglycerides, concomitant with an increase in insulin resistance (*Figure* S3). Interestingly, three proteins did not show any functional association with the network under our conditions, namely, Teneurin 4 (see *Figure* 2), Proteoglycan 4, a component of the extracellular

matrix of cartilage, and Attractin, a protein expressed in many tissues including skeletal muscle.[27] Detailing the changes in each subject (BR10/BR0) IgGFc-binding protein, secreted phosphoprotein 24 and Teneurin 4 had the largest increases in abundance (>4-fold) (*Figure* 3D).

Subject-centric correlation between muscle atrophy and plasma proteome

We previously measured muscle atrophy at BR10 in this bed rest cohort.[16] We observed that seven subjects developed muscle atrophy amounting from 4% up to 12.2% loss of quadriceps volume during 10 days of bed rest. Three subjects were relatively atrophy resistant, displaying a corresponding quadriceps volume change of 0.5–1.9% at BR0 compared with BR0 (*Figure* 4A). This was confirmed measuring the difference in fibre cross-sectional area (CSA) in the muscle biopsies of these two groups of subjects. A 7.7% decrease of the median fibre CSA was measured in the fibres of the seven subjects developing muscle atrophy. Conversely, the fibres of the three atrophy-resistant subjects showed essentially no median CSA decrease at BR10 (*Figure* 4B). The heterogeneity of individual responses to bed rest in terms of muscle atrophy and bone loss has been documented in previous studies.[28] The plasma proteome of atrophy-prone and atrophy-resistant subjects at BR0 showed no significant difference, although complement factor H-related protein 3 (CFHR3) had a clear tendence to over two-fold higher expression in atrophy-prone subjects (*Figure* 4C). However, the same comparison at BR10 highlighted four proteins expressed at higher level in atrophy-resistant subjects and two expressed at higher level in atrophy-prone subjects. Haptoglobin-related protein (HPR), apolipoproteins AI and AIV (APOA1, APOA4) and transthyretin (TTR) were more abundant in the plasma of atrophy-resistant subjects, suggesting that higher plasma abundance of these proteins may have a positive correlation with the preservation of muscle mass. Conversely, inter-alpha-trypsin inhibitor H3 (ITIH3) and complement factor H (CFH) displayed higher abundance in the plasma of subjects undergoing larger loss of muscle mass during bed rest, indicating a negative correlation with muscle trophism (*Figure* 4D).

We reasoned that, if these proteins relay the loss vs maintenance of muscle mass occurring in these two groups of subjects, they might also be common to other contexts in which muscle atrophy occurs. For this purpose, we analysed the serum proteome of a cohort of 14 cancer patients with or without cachexia and 14 age-matched controls. We quantified 390 proteins in total, ranging from 223 to 278 in different subjects (*Table* S3). Contamination from red blood cells and platelets were minor (*Figure* S4A,B). We carried out ANOVA and post hoc tests comparing control subjects with cancer patients with and without cachexia. This analysis retrieved 24
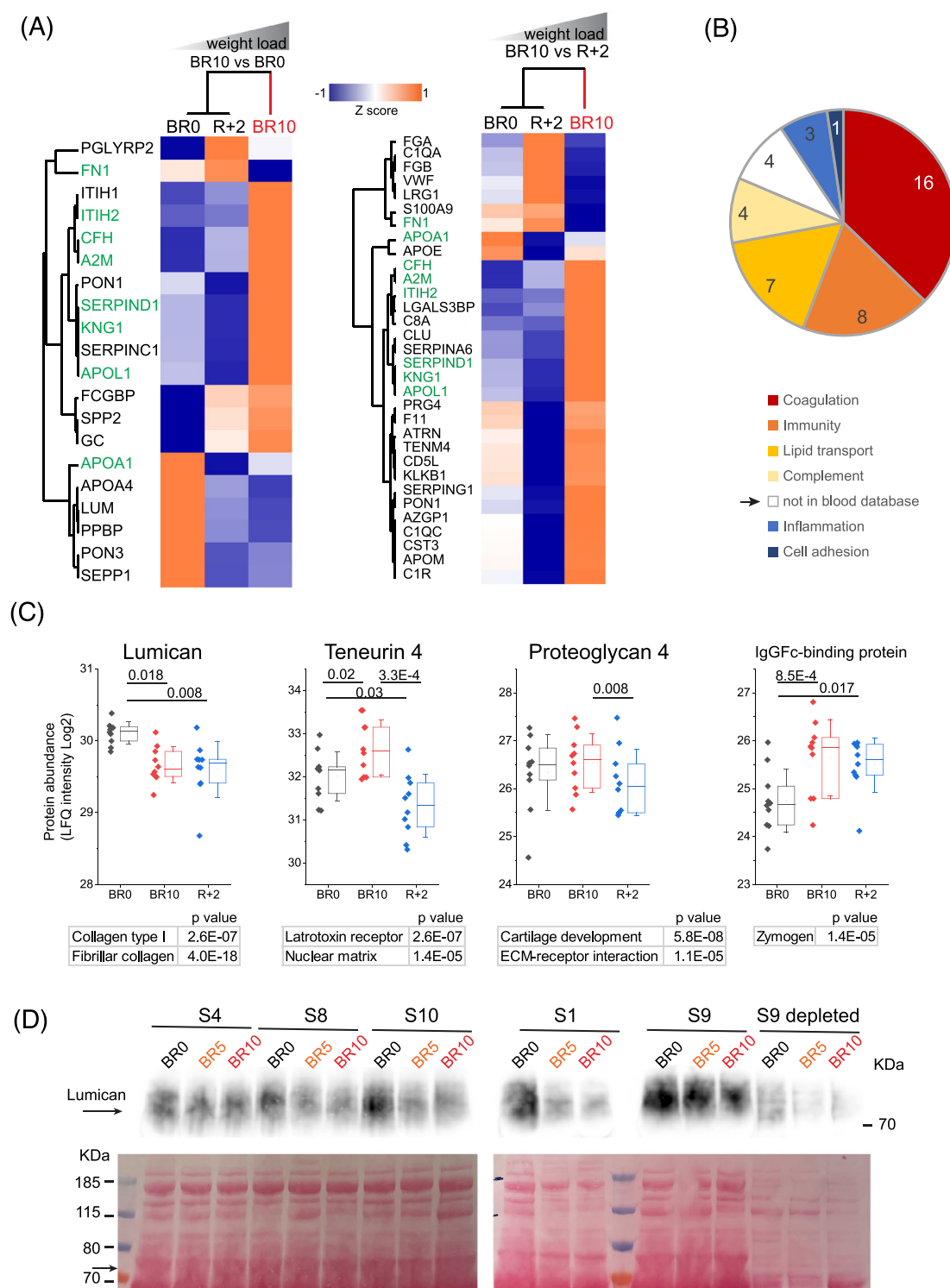
Figure 2 Proteins whose abundance in plasma varied at different loading conditions. (A) Unsupervised hierarchical clustering of proteins that changed significantly in different loading conditions between at least two time points (paired *t*-test, *N* = 10 subjects, permutation-based FDR = 0.05). (B) Main cell compartment or functional class distribution of among ANOVA significant proteins (in percent). From GO terms, manually curated. (C) Plasma abundance changes at different phases of the bed rest protocol of four proteins not of blood origin (see arrows in C) likely originating from tissue leakage. Student's *t*-test, *N* = 10. (D) Top, western blots showing a decreased abundance of Lumican in whole plasma of five subjects (S, see label on top) at BR5 (not analysed by MS-based proteomics) and BR10, matching the results in (C). For S9, Lumican expression after depletion of the 12 most abundant proteins is also shown (top right, last three lanes. Bottom, Ponceau S staining of the upper part of the corresponding membrane). The position of the Lumican band is indicated by an arrow.
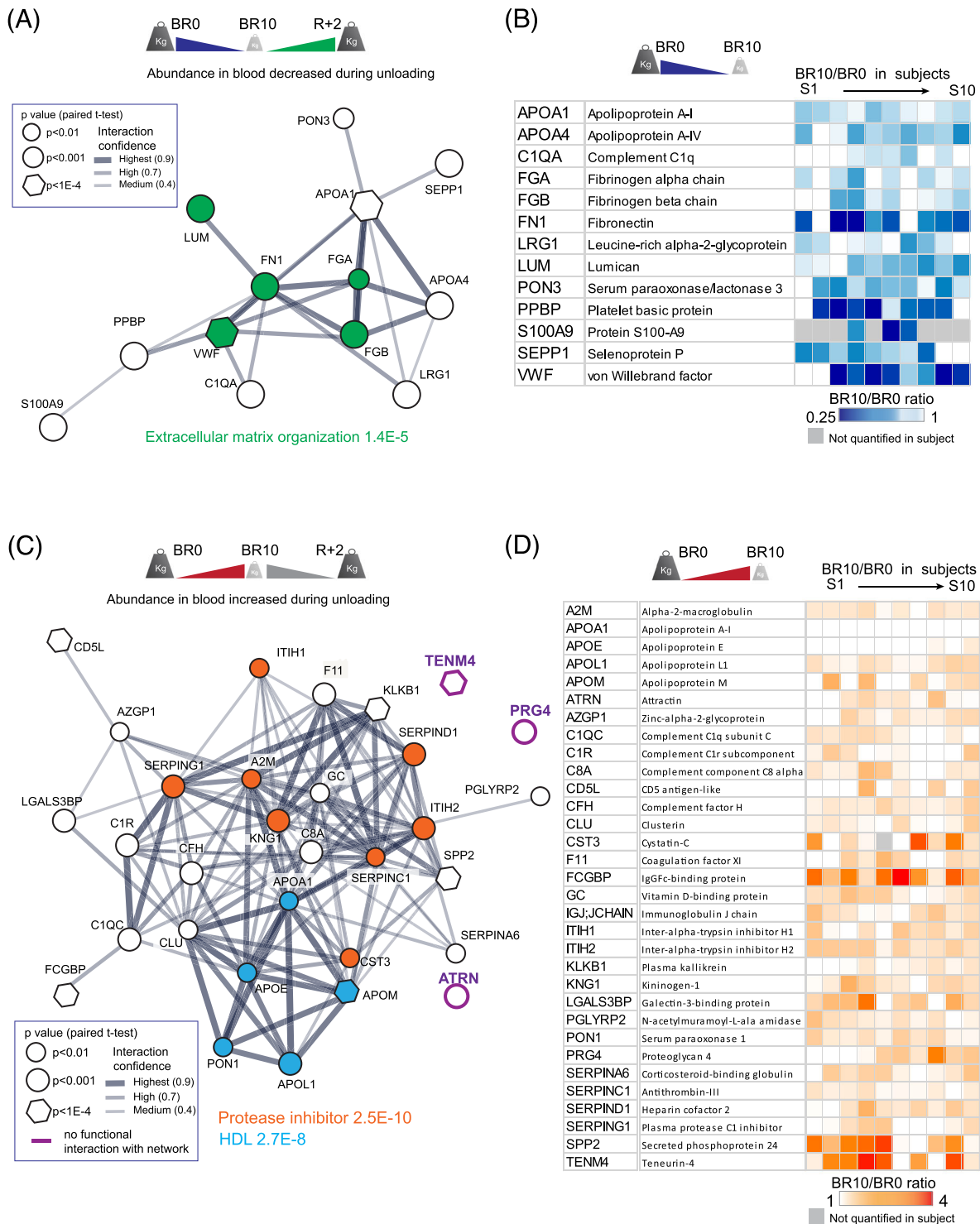
Figure 3 Functional interactions of plasma proteins changing in abundance according to loading conditions. (A) Functional interaction network of proteins whose abundance in plasma decreases during unloading (schematically represented on top). Thickness of connecting lines represents interaction confidence. Node shape is determined by the *P* value of ANOVA. Colours refer to the two most enriched annotations as indicated. See methods for details. (B) Subject-centric heatmap analysis of the decrease in abundance between BR10 and BR0 (BR10/BR0 ratio). Each square shows the median ratio (BR10/BR0) in each of the 10 subjects ordered from S1 to S10, left to right as indicated on top. (C) Functional interaction network of proteins whose abundance in plasma increases during unloading (see A for description). (D) Subject-centric heatmap analysis of the increase in abundance between BR10 and BR0.
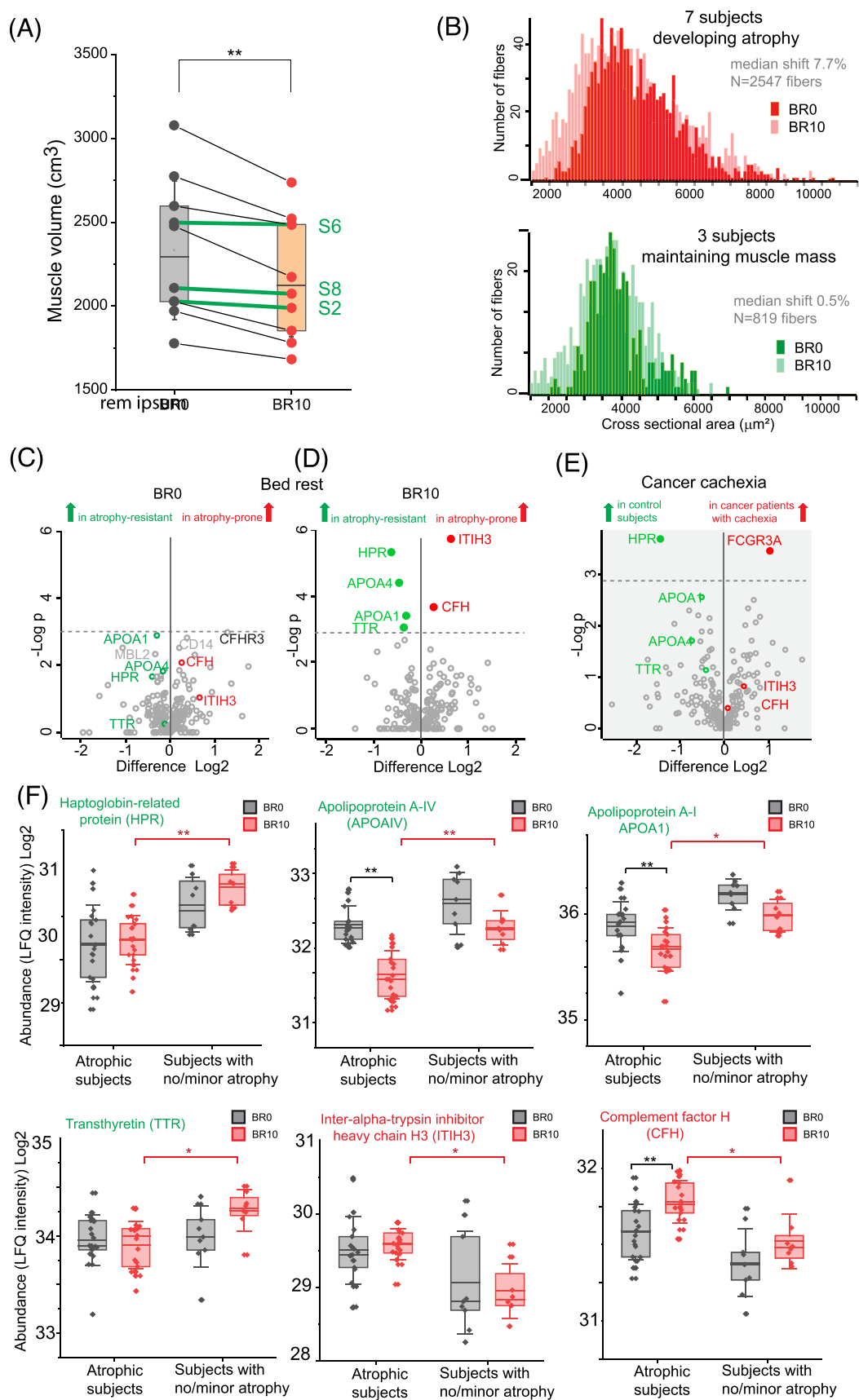
Figure 4 Common features of muscle atrophy in bed rest and cancer cachexia. (A) Bed rest-dependent volume changes of quadriceps femoris at BR0 (black dots) and BR10 (red dots) measured by magnetic resonance imaging (MRI). Three subjects developing no or minor atrophy are indicated by green lines. *N* = 10 subjects. Box shows median, 75th and 25th percentile; whiskers show standard deviation. (B) Distribution of muscle fibre cross-sectional area overlaying BR0 (dark) and BR10 (light). Top, in red, all fibres measured in the muscle biopsies of seven subjects that developed muscle atrophy during bed rest (*N* = 2547 fibres). Bottom, in green, the same analysis for subjects S2, S6 and S8 (see A) that were largely atrophy-resistant (*N* = 819 fibres). (C) Volcano plot comparing the plasma proteome of atrophy-prone and atrophy-resistant bed rest subjects at BR0. In red and green, proteins with significant abundance difference between the subjects at day 10. *N* = 3 atrophy-resistant and 7 atrophy-prone subjects, technical triplicates. Dashed line, *P* value 0.05. Threshold, permutation-based FDR = 0.05. (D) Same analysis as in (C), BR10. Proteins with significantly different abundance between atrophy-resistant and atrophy-prone subjects are labelled with a filled circle. (E) Volcano plot comparing the serum proteome of cancer patients with cachexia (*N* = 7) with that of controls (*N* = 14). Proteins with significantly different abundance between these groups are labelled in colour with a filled circle above the dashed line marking *P* value = 0.05. Proteins with significantly different abundance in the bed rest dataset at day 10 are labelled in colour. (F) Expression of the six proteins with differential expression at BR10 between the seven atrophy-prone (left side of each graph, technical triplicates) and the three atrophy-resistant subjects (right side of each graph, technical triplicates). The red line with asterisks shows the significant differences at BR10 between the two groups of subjects. The black line shows significant differences between BR0 (in black) and BR10 (in red) within the two subject groups. *N* = 10 subjects with two to three technical replicates. **P* < 0.05, ***P* < 0.01. Box shows median, mean, 75th and 25th percentile; whiskers show standard deviation.

proteins whose abundance in plasma differed between at least one of the three groups. Unsupervised hierarchical clustering separated control from cancer patients and the significant hits formed three distinct clusters (*Figure* S4C).

We then compared the serum proteome of control subjects with that of cancer patients that had developed cachexia, leading to the loss of over 5% of their body weight (*Table* S2). Similar to the results obtained in bed rest, HPR was significantly more abundant in the serum of controls compared with that of cachectic cancer patients (*Figure* 4E). This shows that HPR abundance in plasma/serum decreased in subjects losing muscle mass both because of mechanical unloading in young healthy subjects and of cachexia in cancer patients, two scenarios with very few common aspects. Cancer patients significantly up-regulated the receptor for the invariable Fc fragment of immunoglobulin gamma FCGR3A, which was part of a regulated protein cluster in bed rest (see *Figure* 3D and S2). Interestingly, the remaining proteins with higher abundance in atrophy-resistant bed rest subjects also tended to be more abundant in controls compared with cancer patients (compare *Figure* 4D,E, labelled in green). A similar analysis of the serum of controls and cancer patients classified clinically as having pre-cachexia yielded a different set of significant proteins, and the expression difference between the two groups was small (*Figure* S4D). Interestingly, ITIH3, a member of inter-alpha-trypsin inhibitor protein family, was more abundant in the plasma of bed rest subjects at BR10 as well as in the serum of cancer patients with cachexia, correlating in both cohorts with an atrophy state (*Figure* 4D,E).

A plasma protein with significantly different abundance at BR0 between atrophy-prone and atrophy-resistant subjects could be explored as a predictive biomarker. No plasma protein had this behaviour (at a *P* value cut-off of 0.05) in our bed rest cohort (*Figure* 4C). We then focused on the analysis of the six plasma proteins correlated with maintenance or loss of muscle mass at BR10. Interestingly, all but TTR had a tendence to different median expression levels at BR0 in

subject developing muscle atrophy compared with those essentially resistant to it (*Figure* 4F; compare grey boxes). All of them had significantly different expression at BR10 as expected (see also *Figure* 4D).

Discussion

We applied MS-based proteomics to the analysis of plasma samples from a cohort of 10 participants in a bed rest study, undergoing muscle atrophy varying from 12 to 0.4% (quadriceps femoris volume) in 10 days.[5,16] With this approach, we aimed at correlating the loss of muscle mass with changes in abundance of plasma proteins, which could be used to monitor the state of skeletal muscle in a minimally invasive way. We could quantify over 500 proteins in total, amounting to 360 on average in each subject.

Our results revealed over 30 proteins undergoing abundance changes in plasma comparing BR10, the endpoint of mechanical unloading, with BR0, the time point immediately before bed rest. Interestingly, four of the significant proteins were not typical blood components but possibly deriving from tissue leakage. One of them, Teneurin 4, is part of an evolutionarily conserved protein family located predominantly at the synapse.[25] We have previously shown that the subjects of this cohort showed neuromuscular instability, as indicated by the up-regulation of neural cell adhesion molecule 1 (NCAM) in skeletal muscle, a marker of denervation/re-innervation events.[16] It will be of interest to test Teneurin 4 as a readout for NMJ instability. Proteoglycan 4 (PRG4)/lubricin is a cartilage protein whose serum abundance increases in patients with active inflammatory cartilage disease.[29] We detected a minor increase in the plasma abundance of PRG4 during bed rest, but a significant twofold decrease 2 days after reloading. Lumican, a protein enriched in the extracellular matrix of articular cartilage, was more abundant at BR0 than at both BR10 and BR5, as we could

show in validation experiments using western blot. It could be speculated that variations in loading cause extensive re-modelling of cartilage, leading to changes in plasma abundance of extracellular matrix proteins.[30]

In addition, we found significant decrease in abundance at BR10 for proteins involved in interactions with the extracellular matrix and in blood coagulation. Long hospitalizations are linked to a hypercoagulable state and to increased risk of thromboembolic complications. However, in line with our findings, previous bed rest studies in healthy young subjects have observed no increase in major coagulation parameters during 21 days[31] or 60 days of head down tilt bed rest.[32] Indeed, both studies reported a tendence to a hypocoagulable state during bed rest, which would work as a compensatory mechanism. Our results show that the abundance of some plasma apolipoproteins was higher at BR10 compared with BR0, including APOA1, whose plasma concentration was not modified by inactivity in other studies.[33] These changes may be due to the inactivity-linked insulin resistance that we and others have consistently observed starting in the early phases of bed rest.[34] Insulin resistance causes lipoprotein lipase inhibition and activation of hepatic triglyceride synthase, which are known to cause significant changes in blood lipid profile.[35] Inhibitors of different protease families, including anti-trypsin, anti-thrombin and anti-C3, were more abundant at BR10 compared with BR0. Members of the inter-alpha-trypsin family have been recently suggested to associate with mortality in COVID-19. ITIH3 and ITIH1/2 showed opposite differences in abundance between survivors and non-survivors.[36] Our data confirm opposite changes of different members of this protein family, both in subjects undergoing bed rest and in cancer patients (see below).

Interindividual differences in the response to intervention (e.g. lifestyle of pharmacological) are the theoretical basis for personalized medicine, which is rapidly developing with the support of large throughput data generated with omics technologies. The ability to predict different impacts of inactivity with minimally invasive methods would be of great interest to monitor community health and design early intervention, particularly in the elderly population. In the future, biomarkers predicting a muscle atrophy-resistant phenotype might be of paramount importance for the selection of astronauts for long space missions, where body unloading due to microgravity represents a severe challenge for human health.[37] A serendipitous finding of our previous analysis of this bed rest subject cohort was significant inter-individual heterogeneity in the susceptibility to unloading-induced muscle atrophy, consistent with previous reports.[28] Whereas seven subjects lost between 4% and 12.2% of their quadriceps volume in 10 days, three of them had minor decreases, from 1.9 to 0.4%. Comparing the abundance of plasma proteins in atrophy-prone and atrophy-resistant subjects at BR10, we highlighted six proteins showing significant differences between the two groups. Two proteins were more

abundant in subjects developing atrophy during bed rest, namely, the protease inhibitor ITIH3 and complement factor H (CFH). Four proteins, haptoglobin-related protein (HPR), transthyretin (TTR) and the apolipoproteins APOA1 and APOA2 were more abundant in atrophy-resistant subjects. Interestingly from a biomarker perspective, the abundance difference was the same at BR10 as at BR0, though only the samples at BR10 reached statistical significance under our conditions (compare *Figure* 4C,D). It will be of interest to further evaluate the ability of these proteins, alone or in combination, to predict the proneness to muscle atrophy in different subjects.

To further evaluate the relationship between loss of muscle mass and changes in circulating proteins, we analysed the serum of seven cancer patients with cachexia, leading to over 8% loss of total body weight. The comparison between the serum of cachectic patients and that of controls yielded two significant proteins. The receptor for the invariable Fc fragment of immunoglobulin gamma FCGR3A/CD16A, a cytotoxicity receptor of human natural killer (NK) cells,[38] was more abundant in cancer patients with cachexia. This might be linked to the disease phenotype, though the functional annotation FCGR activation was also regulated in bed rest (*Figure* S2). Interestingly, haptoglobin-related protein/HPR was over twofold more abundant in the serum of controls compared with cancer patients with cachexia.

Crossing the results of the bed rest and cancer cachexia cohort, we thus show that the level of circulating haptoglobin-related protein/HPR correlates with the maintenance of muscle mass in both conditions inducing skeletal atrophy, despite the large differences characterizing the two subject groups. Although HPR has been proposed as a serum marker of lymphoma,[39] the abundance of HPR does not result different when we compare the serum cancer patient without cachexia with that of controls (*Figure* S4D). Our analysis points to a positive correlation between circulating HPR and muscle mass.

Despite suggesting a number of circulating potential biomarkers of muscle atrophy, our study presents several limitations that need to be taken into account. The bed rest dataset lacks an intermediate time point. As a consequence, our proteomic data do not show how these potential biomarkers change over time and whether they occur in the early phase of bed rest, where most of the signal transduction controlling atrophy unfolds, or whether they manifest towards the end of the bed rest sequence, where atrophy is most pronounced. For Lumican, we could show by western blot that the plasma abundance is already decreased at BR5 and maintained at a low level at BR10. Our pilot study is also limited in sample size, so our findings will need further validation in larger cohorts. At this stage, our result cannot yet contribute practical predictive power to the indirect methods used to assess muscle atrophy, like grip strength or body weight measurements. However, this detailed quantification of the plasma

\proteome, together with the characterization of the skeletal muscle of the same bed rest cohort from our parallel studies,[16,40] will allow to draw correlations and perform data mining once larger validation cohorts have been analysed.

In conclusion, we found changes in the plasma proteome of healthy subjects undergoing voluntary bed rest that accompany and may be linked to the mechanical loading/activity state of the body and to muscle trophism. In the future, this type of studies validated in large cohorts will lead to the definition of biomarkers panels relaying information on skeletal muscle trophism, contributing to the development of point-of-care diagnostics for human health.

Acknowledgements

Conflict of interest

The authors declare no conflict of interest.

Online supplementary material

Additional supporting information may be found online in the Supporting Information section at the end of the article.

References

1. Cruz-Jentoft AJ, Sayer AA. Sarcopenia. *Lancet* 2019;**393**:2636–2646.
2. Fearon K, Strasser F, Anker SD, Bosaeus I, Bruera E, Fainsinger RL, Jatoi A, Loprinzi C, MacDonald N, Mantovani G, Davis M, Muscaritoli M, Ottery F, Radbruch L, Ravasco P, Walsh D, Wilcock A, Kaasa S, Baracos VE. Definition and classification of cancer cachexia: an international consensus. *Lancet Oncol* 2011;**12**:489–495.
3. Argiles JM, Busquets S, Stemmler B, Lopez-Soriano FJ. Cancer cachexia: understanding the molecular basis. *Nat Rev Cancer* 2014;**14**:754–762.
4. Kilroe SP, Fulford J, Jackman S, Holwerda A, Gijsen A, van Loon L, Wall BT. Dietary protein intake does not modulate daily myofibrillar protein synthesis rates or loss of muscle mass and function during short-term immobilization in young men: a randomized controlled trial. *Am J Clin Nutr* 2021;**113**:548–561.
5. Franchi MV, Sarto F, Simunic B, Pisot R, Narici MV. Early changes of hamstrings morphology and contractile properties during 10 days of complete inactivity. *Med Sci Sports Exerc* 2022;**54**:1346–1354.
6. Šimunič B, Koren K, Rittweger J, Lazzer S, Reggiani C, Rejc E, Pišot R, Narici M, Degens H. Tensiomyography detects early hallmarks of bed-rest-induced atrophy before changes in muscle architecture. *J Appl Physiol* 2019;**126**:815–822.
7. Sartori R, Romanello V, Sandri M. Mechanisms of muscle atrophy and hypertrophy: implications in health and disease. *Nat Commun* 2021;**12**:330.
8. Bodine SC, Latres E, Baumhueter S, Lai VK, Nunez L, Clarke BA, Poueymirou WT, Panaro FJ, Na E, Dharmarajan K, Pan ZQ, Valenzuela DM, DeChiara TM, Stitt TN, Yancopoulos GD, Glass DJ. Identification of ubiquitin ligases required for skeletal muscle atrophy. *Science* 2001;**294**:1704–1708.
9. Sandri M, Sandri C, Gilbert A, Skurk C, Calabria E, Picard A, Walsh K, Schiaffino S, Lecker SH, Goldberg AL. Foxo transcription factors induce the atrophy-related ubiquitin ligase atrogin-1 and cause skeletal muscle atrophy. *Cell* 2004;**117**:399–412.
10. Hughes DC, Baehr LM, Driscoll JR, Lynch SA, Waddell DS, Bodine SC. Identification and characterization of Fbxl22, a novel skeletal muscle atrophy-promoting E3 ubiquitin ligase. *Am J Physiol Cell Physiol* 2020;**319**:C700–C719.
11. Masiero E, Agatea L, Mammucari C, Blaauw B, Loro E, Komatsu M, Metzger D, Reggiani C, Schiaffino S, Sandri M. Autophagy is required to maintain muscle mass. *Cell Metab* 2009;**10**:507–515.
12. Tezze C, Romanello V, Desbats MA, Fadini GP, Albiero M, Favaro G, Ciciliot S, Soriano ME, Morbidoni V, Cerqua C, Loefler S, Kern H, Franceschi C, Salvioli S, Conte M, Blaauw B, Zampieri S, Salviati L, Scorrano L, Sandri M. Age-associated loss of OPA1 in muscle impacts muscle mass, metabolic homeostasis, systemic inflammation, and xepithelial senescence. *Cell Metab* 2017;**25**:1374–1389.e6.
13. Cohen S, Nathan JA, Goldberg AL. Muscle wasting in disease: molecular mechanisms and promising therapies. *Nat Rev Drug Discov* 2015;**14**:58–74.
14. Richter EA, Hargreaves M. Exercise, GLUT4, and skeletal muscle glucose uptake. *Physiol Rev* 2013;**93**:993–1017.
15. Rittweger J, Albracht K, Flück M, Ruoss S, Brocca L, Longa E, Moriggi M, Seynnes O, di Giulio I, Tenori L, Vignoli A, Capri M, Gelfi C, Luchinat C, Franceschi C, Bottinelli R, Cerretelli P, Narici M. Sarcolab pilot study into skeletal muscle's adaptation to long-term spaceflight. *NPJ Microgravity* 2018;**4**:18.
16. Monti E, Reggiani C, Franchi MV, Toniolo L, Sandri M, Armani A, Zampieri S, Giacomello E, Sarto F, Sirago G, Murgia M, Nogara L, Marcucci L, Ciciliot S, Šimunic B, Pišot R, Narici MV. Neuromuscular junction instability and altered intracellular calcium handling as early determinants of force loss during unloading in humans. *J Physiol* 2021;**599**:3037–3061.
17. Lim S, Dunlap KR, Rosa-Caldwell ME, Haynie WS, Jansen LT, Washington TA, et al. Comparative plasma proteomics in muscle atrophy during cancer-cachexia and disuse: the search for atrokines. *Physiol Rep* 2020;**8**:e14608.
18. Sartori R, Hagg A, Zampieri S, Armani A, Winbanks CE, Viana LR, Haidar M, Watt KI, Qian H, Pezzini C, Zanganeh P, Turner BJ,

Larsson A, Zanchettin G, Pierobon ES, Moletta L, Valmasoni M, Ponzoni A, Attar S, da Dalt G, Sperti C, Kustermann M, Thomson RE, Larsson L, Loveland KL, Costelli P, Megighian A, Merigliano S, Penna F, Gregorevic P, Sandri M. Perturbed BMP signaling and denervation promote muscle wasting in cancer cachexia. *Sci Transl Med* 2021;**13**.

19. Hortin GL, Sviridov D, Anderson NL. High-abundance polypeptides of the human plasma proteome comprising the top 4 logs of polypeptide abundance. *Clin Chem* 2008;**54**:1608–1616.

20. Geyer PE, Voytik E, Treit PV, Doll S, Kleinhempel A, Niu L, et al. Plasma proteome profiling to detect and avoid sample-related biases in biomarker studies. *EMBO Mol Med* 2019;**11**:e10427.

21. Cox J, Mann M. MaxQuant enables high peptide identification rates, individualized p.p.b.-range mass accuracies and proteome-wide protein quantification. *Nat Biotechnol* 2008;**26**:1367–1372.

22. Tyanova S, Temu T, Sinitcyn P, Carlson A, Hein MY, Geiger T, Mann M, Cox J. The Perseus computational platform for comprehensive analysis of (prote)omics data. *Nat Methods* 2016;**13**:731–740.

23. Cox J, Hein MY, Luber CA, Paron I, Nagaraj N, Mann M. Accurate proteome-wide label-free quantification by delayed normalization and maximal peptide ratio extraction, termed MaxLFQ. *Mol Cell Proteomics* 2014;**13**:2513–2526.

24. Uhlén M, Karlsson MJ, Hober A, Svensson AS, Scheffel J, Kotol D, Zhong W, Tebani A, Strandberg L, Edfors F, Sjöstedt E, Mulder J, Mardinoglu A, Berling A, Ekblad S, Dannemeyer M, Kanje S, Rockberg J, Lundqvist M, Malm M, Volk AL, Nilsson P, Månberg A, Dodig-Crnkovic T, Pin E, Zwahlen M, Oksvold P, von Feilitzen K, Häussler RS, Hong MG, Lindskog C, Ponten F, Katona B, Vuu J, Lindström E, Nielsen J, Robinson J, Ayoglu B, Mahdessian D, Sullivan D, Thul P, Danielsson F, Stadler C, Lundberg E, Bergström G, Gummesson A, Voldborg BG, Tegel H, Hober S, Forsström B, Schwenk JM, Fagerberg L, Sivertsson Å. The human secretome. *Sci Signal* 2019;**12**.

25. Tucker RP. Teneurins: domain architecture, evolutionary origins, and patterns of expression. *Front Neurosci* 2018;**12**:938.

26. Chawla K, Ham HO, Nguyen T, Messersmith PB. Molecular resurfacing of cartilage with proteoglycan 4. *Acta Biomater* 2010;**6**:3388–3394.

27. Ehara A, Taguchi D, Nakadate K, Ueda S. Attractin deficiency causes metabolic and morphological abnormalities in slow-twitch muscle. *Cell Tissue Res* 2021;**384**:745–756.

28. Bocker J, Schmitz MT, Mittag U, Jordan J, Rittweger J. Between-subject and within-subject variation of muscle atrophy and bone loss in response to experimental bed rest. *Front Physiol* 2022;**12**:743876.

29. Kisla Ekinci RM, Balcı S, Coban F, Bisgin A. Serum lubricin levels in patients with juvenile idiopathic arthritis. *Reumatologia* 2021;**59**:373–377.

30. Yokota H, Leong DJ, Sun HB. Mechanical loading: bone remodeling and cartilage maintenance. *Curr Osteoporos Rep* 2011;**9**:237–242.

31. Cvirn G, Waha JE, Ledinski G, Schlagenhauf A, Leschnik B, Koestenberger M, Tafeit E, Hinghofer-Szalkay H, Goswami N. Bed rest does not induce hypercoagulability. *Eur J Clin Invest* 2015;**45**:63–69.

32. Venemans-Jellema A, Schreijer AJ, le Cessie S, Emmerich J, Rosendaal FR, Cannegieter SC. No effect of isolated long-term supine immobilization or profound prolonged hypoxia on blood coagulation. *J Thromb Haemost* 2014;**12**:902–909.

33. Yanagibori R, Suzuki Y, Kawakubo K, Kondo K, Iwamoto T, Itakura H, Makita Y, Sekiguchi C, Gunji A, Kondou K. The effects of 20 days bed rest on serum lipids and lipoprotein concentrations in healthy young subjects. *J Gravit Physiol* 1997;**4**:S82–S90.

34. Mikines KJ, Richter EA, Dela F, Galbo H. Seven days of bed rest decrease insulin action on glucose uptake in leg and whole body. *J Appl Physiol* 1991;**70**:1245–1254.

35. Bey L, Hamilton MT. Suppression of skeletal muscle lipoprotein lipase activity during physical inactivity: a molecular reason to maintain daily low-intensity activity. *J Physiol* 2003;**551**:673–682.

36. Vollmy F, van den Toorn H, Zenezini Chiozzi R, Zucchetti O, Papi A, Volta CA, et al. A serum proteome signature to predict mortality in severe COVID-19 patients. *Life Sci Alliance* 2021;**4**.

37. Garrett-Bakelman FE, Darshi M, Green SJ, Gur RC, Lin L, Macias BR, McKenna MJ, Meydan C, Mishra T, Nasrini J, Piening BD, Rizzardi LF, Sharma K, Siamwala JH, Taylor L, Vitaterna MH, Afkarian M, Afshinnekoo E, Ahadi S, Ambati A, Arya M, Bezdan D, Callahan CM, Chen S, Choi AMK, Chlipala GE, Contrepois K, Covington M, Crucian BE, de Vivo I, Dinges DF, Ebert DJ, Feinberg JI, Gandara JA, George KA, Goutsias J, Grills GS, Hargens AR, Heer M, Hillary RP, Hoofnagle AN, Hook VYH, Jenkinson G, Jiang P, Keshavarzian A, Laurie SS, Lee-McMullen B, Lumpkins SB, MacKay M, Maienschein-Cline MG, Melnick AM, Moore TM, Nakahira K, Patel HH, Pietrzyk R, Rao V, Saito R, Salins DN, Schilling JM, Sears DD, Sheridan CK, Stenger MB, Tryggvadottir R, Urban AE, Vaisar T, van Espen B, Zhang J, Ziegler MG, Zwart SR, Charles JB, Kundrot CE, Scott GBI, Bailey SM, Basner M, Feinberg AP, Lee SMC, Mason CE, Mignot E, Rana BK, Smith SM, Snyder MP, Turek FW. The NASA twins study: a multidimensional analysis of a year-long human spaceflight. *Science* 2019;**364**.

38. Zhu H, Blum RH, Bjordahl R, Gaidarova S, Rogers P, Lee TT, Abujarour R, Bonello GB, Wu J, Tsai PF, Miller JS, Walcheck B, Valamehr B, Kaufman DS. Pluripotent stem cell-derived NK cells with high-affinity noncleavable CD16a mediate improved antitumor activity. *Blood* 2020;**135**:399–410.

39. Epelbaum R, Shalitin C, Segal R, Valansi C, Arselan I, Faraggi D, Leviov M, Ben-Shahar M, Haim N. Haptoglobin-related protein as a serum marker in malignant lymphoma. *Pathol Oncol Res* 1998;**4**:271–276.

40. Murgia M, Ciciliot S, Nagaraj N, Reggiani C, Schiaffino S, Franchi MV, et al. Signatures of muscle disuse in spaceflight and bed rest revealed by single muscle fiber proteomics. *PNAS Nexus* 2022;**1**.

41. von Haehling S, Morley JE, Coats AJS, Anker SD. Ethical guidelines for publishing in the Journal of Cachexia, Sarcopenia and Muscle: update 2021. *J Cachexia Sarcopenia Muscle* 2021;**12**:2259–2261.